In Situ Microfibrillar-Reinforced Composites of Isotactic Polypropylene/Recycled Poly(ethylene terephthalate) System and Effect of Compatibilizer

Pattama Taepaiboon,[1] Jirawut Junkasem,[1] Rapeephun Dangtungee,[1] Taweechai Amornsakchai,[2] Pitt Supaphol[1]

[1]*The Petroleum and Petrochemical College, Chulalongkorn University, Bangkok 10330, Thailand*
[2]*Department of Chemistry, Faculty of Science, Mahidol University, Bangkok 10400, Thailand*

Received 14 June 2005; accepted 4 March 2006
DOI 10.1002/app.24402
Published online in Wiley InterScience (www.interscience.wiley.com).

ABSTRACT: Recycled poly(ethylene terephthalate) from waste bottles (hereafter, rPET) was used as an reinforcing material for isotactic polypropylene (iPP) based on the concept of *in situ* microfibrillar-reinforced composites (iMFCs). Microfibers of rPET were successfully generated during melt-extrusion and subsequent drawing and preserved in the final injection-molded specimens. The effects of draw ratio, initial size of ground rPET flakes, and rPET content on morphological appearance of the extrudates and the as-formed rPET fibers and mechanical properties of the as-prepared iMFCs were investigated. The results showed that diameters of the as-formed rPET fibers decreased with increasing draw ratio, and the initial size of ground rPET flakes did not affect the final diameters of the as-formed rPET fibers nor the mechanical properties of the as-prepared iMFCs. Flexural modulus, tensile modulus, and tensile strength of iPP/rPET iMFCs were improved by the presence of rPET microfibers and further improvement could be achieved by the addition of maleic anhydride-grafted iPP (PP-*g*-MA), which was used as the compatibilizer. © 2006 Wiley Periodicals, Inc. J Appl Polym Sci 102: 1173–1181, 2006

Key words: recycling; reinforced composites; isotactic polypropylene; poly(ethylene terephthalate)

INTRODUCTION

Since the introduction of poly(ethylene terephthalate) (PET) in 1953, commercial utilization of this polymer has been growing continuously. One of the main applications for PET is in the area of packaging, where optical clarity is the main concern. In most parts of the world, majority of the postconsumer material converts into plastic wastes, which usually find their way to a landfill. In developed industrial countries, however, reuse and recycling of the plastic wastes or conversion of them into energy are common practices. Nonetheless, recycling of PET is quite common in the industry.[1] Recycled PET (rPET) has been used as a component in the production of parts and textile for automobiles and as a cost-reduction ingredient for food containers.[1] An alternative way for making use of rPET proposed in the present contribution is to blend rPET with a polyolefin, based on the concept of *in situ* microfibrillar-reinforced composites (iMFCs).[2]

IMFCs are different from the classical composites and conventional blends in that microfibrillar structure of the reinforcing polymer within the polymer matrix is formed during processing. Four elemental steps are envisaged[2] as shown in Figure 1: (1) blending of immiscible polymeric components whose apparent melting temperatures (T_m) differ by at least 30°C (the T_m of the reinforced minor phase is greater), (2) extrusion of the as-prepared blends, (3) drawing the obtained extrudates to fibrillate the minor, dispersed phase, and (4) annealing or isotropization of the as-drawn extrudates above the T_m of the major phase. In addition to the synergistic effects of the resulting mechanical properties, iMFCs offer another important advantage in that the reinforcing element is also a conventional thermoplastic; so, no mineral additives are involved.[1,3]

Many polymeric systems have been explored as the iMFCs. Evstatiev et al.[4] studied and reported the structure–property relationship of microfibrillar-reinforced polyamide-6/PET composites. In a subsequent study, Evstatiev et al.[5] studied and reported the structure–property relationship of microfibrillar-reinforced polyamide-6 and polyamide-66 blend/PET composites. The mechanical properties of iMFCs have been reported to

Correspondence to: P. Supaphol (pitt.s@chula.ac.th).
Contract grant sponsors: Petroleum and Petrochemical Technology Consortium; Petroleum and Petrochemical College, Chulalongkorn University.

© 2006 Wiley Periodicals, Inc.

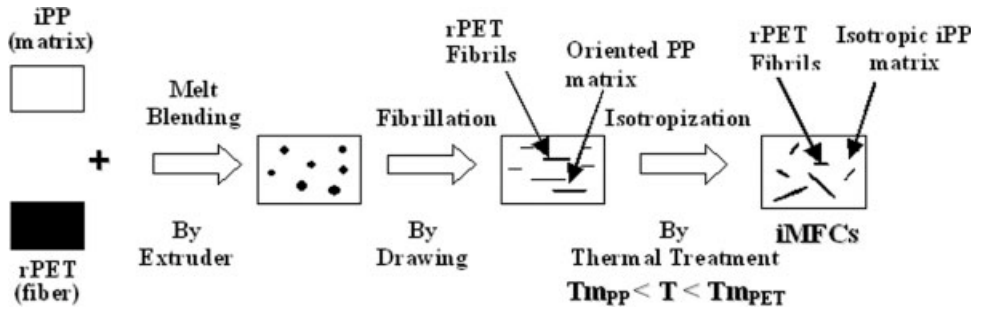

Figure 1 Schematic diagram for preparing iPP/rPET iMFCs.

be quite promising. Li et al.[6] reported that the tensile modulus and tensile strength of polyethylene (PE)/PET iMFCs were significantly increased from those of neat PE and conventional PE/PET blends. Interestingly, Cunha and Fakirov[3] reported in their book that the tensile strength of isotactic polypropylene (iPP)/PET (50/50 w/w) iMFCs was almost four times greater than that of iPP reinforced with 30 wt % of short glass fibers.

Further studies of iMFCs were focused on the use of the compatibilizer. Because of the immiscibility and lack of interfacial adhesion between the dispersed and the matrix phases, an effective compatibilizer is needed to improve the degree of compatibilization between the two phases, which should finally result in an improvement in the mechanical properties of the final composites. In the presence of a compatibilizer, morphology of the resulting blends shows good dispersion of fine minor phase. The improvement of the essential work of fracture of PE/PET iMFCs was reported when ethylene–vinyl acetate copolymer was used as the compatibilizer, with scanning electron micrographs showing a strong interfacial bonding between PET microfibers and PE matrix, rendering the stress being readily transferred from the matrix to the fibers.[7]

In the present contribution, maleic anhydride-grafted polypropylene (PP-*g*-MA) was chosen as the compatibilizer to improve the mechanical properties of iPP/rPET iMFCs. PP-*g*-MA was chosen as the compatibilizer because of its high reactivity and reported successful results based on the study of Yoon et al.,[8] in which they showed that the improvement in the mechanical properties of PET/PP-*g*-MA reactive blends were better than those of PET/iPP conventional blends, a direct result of the improved miscibility between the two phases. The main purposes of the present contribution are, therefore, to investigate the effects of draw ratio, initial size of ground rPET flakes, rPET content, and the addition of PP-*g*-MA on morphological appearance of the extrudates and the as-formed rPET fibers and mechanical properties of the resulting iMFCs.

EXPERIMENTAL

Materials

A commercial grade of iPP (HP400K) was courteously supplied by HMC Polymers Co. (Thailand) in granular form. It was a homopolymer with a density of 0.90 g/cm^3 and a melt-flow rate of 4 dg/min. rPET from waste bottles was purchased from Leingthong Co. (Thailand) in grounded flake form. The grounded rPET flakes were seived into three size ranges, i.e., 0.5–1 mm, 1–2 mm, and >2 mm. Two types of antioxidants, Anox 20 and Alkanox 240 (Great Lakes Chemical Corp.), were kindly supplied by Vicker Pigment Co. (Thailand). PP-*g*-MA (Fusabond MZ203D), used as the compatibilizer between iPP and rPET phases, was courteously supplied by Dupont Co.

Composite preparation

Vacuum-dried (100°C, 24 h) rPET flakes, neat iPP pellets, and PP-*g*-MA pellets were first dry-mixed to produce blends of varying composition ranging between

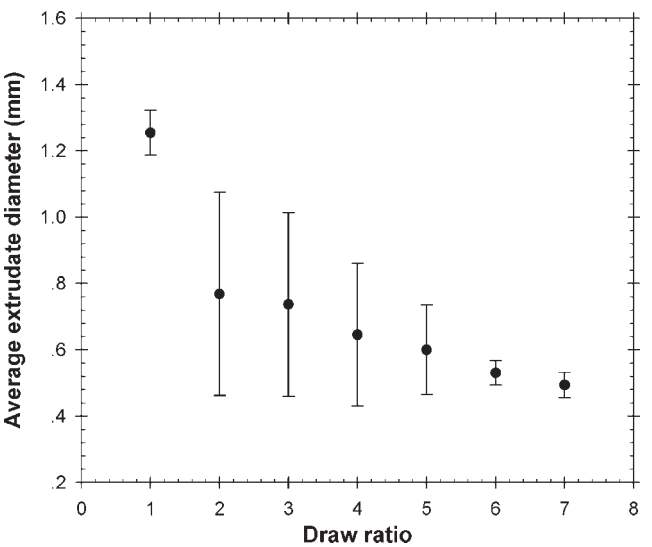

Figure 2 Diameters of as-drawn 85/15 w/w iPP/rPET extrudates as a function of draw ratio.

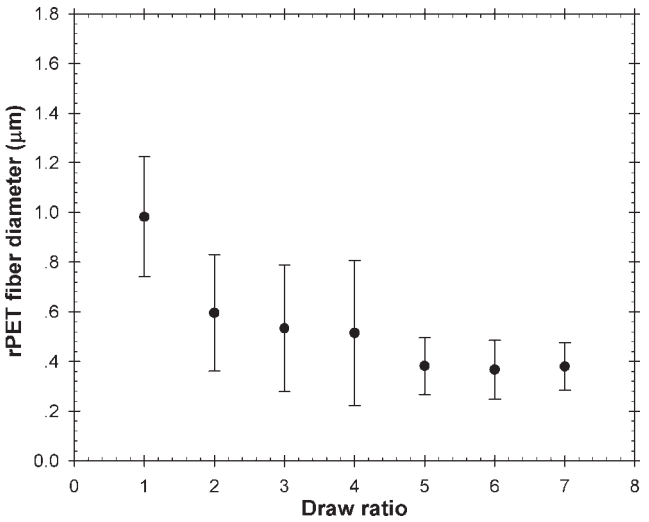

Figure 3 Diameters of rPET fibers formed in as-drawn 85/15 w/w iPP/rPET extrudates as a function of draw ratio.

0 and 30 wt % of rPET and 0 and 7 wt % of PP-*g*-MA, respectively. In this step, 0.1 wt % of Anox 20 and 0.1 wt % of Alkanox 240 were added to prevent extensive thermal degradation of iPP. The dry-mixed blends were then melt-mixed in a Collin ZK25 self-wiping, corotating twin-screw extruder at a fixed screw speed of 45 rpm. The temperature profile (from the feed zone to the die) of the extruder was 130, 210, 240, 260, 270, and 280°C. The diameter of the die opening was 2 mm. The extrudates were continuously collected on a homemade take-up device operating at a constant rotational speed of 400 rpm. The products from this step are hereafter called as-extruded composites.

The extrudates were later drawn between two pinching rolls of equal outside diameters set across a heating tunnel, the temperature of which was set at 90°C. The rotational speed of the leading roller was fixed at 10 rpm and that of the following roller was varied between 20 and 70 rpm, corresponding to a varying draw ratio of about 2–7. The drawn extrudates were then pelletized. Finally, the composite granules were injection-molded into specimens for mechanical testing using an ARBURG Allrounder® 270M injection molding machine. The temperature settings (from the feed zone to the nozzle) were 150, 160, 170, 180, and 185°C, respectively. The injection pressure was 1700 bar and the dwelling pressure was 700 bar. Prior to the mechanical tests, all of the test specimens were conditioned under ambient conditions for 5 days.

Composite characterization

Tensile properties of the iPP/rPET and iPP/rPET iMFCs compatibilized with PP-*g*-MA were tested on an Instron 4206 universal testing machine at room temperature, following the ASTM D638-91 standard test method. The crosshead speed, the gauge length, and the maximum load were 50 mm/min, 50 mm, and 100 kN, respectively. Flexural properties of the as-prepared iMFCs were measured on the Instron 4206 universal testing machine at room temperature according to the ASTM D790 standard test method. The results were reported as average values from at least seven measurements. Impact resistance of the as-prepared iMFCs both with and without PP-*g*-MA was measured on a Zwick 5113 pendulum impact tester according the ASTM D256-90b standard test method. The size of the samples was $12.7 \times 62 \times 4$ mm^3, with a notch being marked on each specimen according to the Izod method. The results were reported as average values from at least 10 measurements.

The morphology of the as-prepared iMFCs both with and without PP-*g*-MA was observed on a JEOL JSM-5200 scanning electron microscope (SEM). Selected as-extruded composites and as-injection-molded impact specimens were cryogenically fractured in the transverse direction to provide a cross-sectional view. The longitudinal view of selected as-extruded composites was obtained by manual splitting of the extrudates. The fractured surfaces were sputtered with a thin layer of gold prior to SEM observation. Based on these SEM images, average diameters of the as-formed rPET fibers were obtained. The results were reported as average values from as least 50 measurements. The outer diameter of the iPP/rPET extrudates was measured by a vernier caliper. The results were reported as average values from at least 50 measurements for every 1 m of each extrudate sample. The diameter of the rPET fibers formed was measured by image analysis of SEM images obtained. The results were reported as average values from at least 50 measurements.

RESULTS AND DISCUSSION

Effect of draw ratio

The diameters of the neat and the as-drawn 85/15 w/w iPP/rPET extrudates were measured by a vernier caliper. The draw ratio was varied between 2 and 7, with the rotational speed of the leading roller being fixed at 10 rpm and that of the follower roller varying between

TABLE I
Effect of Initial Sizes of Ground rPET Flakes on Diameters of rPET Fibers and Some Mechanical Properties of Resulting 85/15 w/w iPP/rPET iMFCs

Size of ground rPET flakes (mm)	rPET fiber diameter[a] (μm)	Tensile modulus (MPa)	Flexural modulus (MPa)	Impact resistance (J/m)
0.5–1	0.36 ± 0.11	1914 ± 204	533 ± 40	34.1 ± 3.0
1–2	0.38 ± 0.10	1951 ± 189	528 ± 43	35.8 ± 2.5
>2	0.38 ± 0.11	1877 ± 209	518 ± 37	34.3 ± 1.8

[a] Diameters of rPET fibers were measured from the as-drawn (draw ratio = 7) iMFC samples.

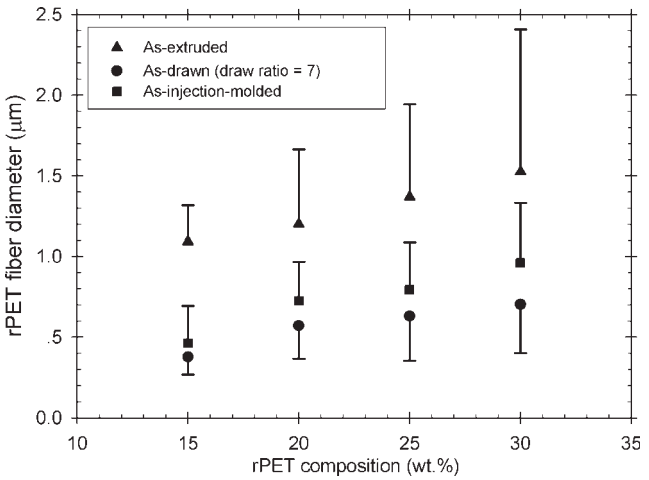

Figure 4 Diameters of rPET fibers formed in iPP/rPET samples collected after various steps (i.e., melt-extrusion, hot-drawing, or injection molding) as a function of rPET composition.

20 and 70 rpm. Obviously, the average diameter of the as-drawn iPP/rPET extrudates was much lower than that of the neat extrudate. Specifically, the average diameter of the as-drawn extrudates decreased from about 1.2 mm for the neat extrudate to about 0.8 mm for the iPP/rPET extrudate, which was drawn at the draw ratio of 2, and decreased gradually with further increase in the draw ratio (see Fig. 2). Interestingly, the distribution of the diameters was also a decreasing function of the draw ratio. Since the drawing process was carried out at a temperature between the glass transition temperature (T_g) and the T_m of both components, it is called a cold-drawing process.[9] The much wide distribution of the extrudate diameters at ''low'' draw ratios was a result of uneven drawing at those draw ratios. A much even drawing was achieved when the draw ratio was between 5 and 7 (see Fig. 2). Here, uneven drawing is characterized by intermittent necking that was observed along the length of the extrudate strand.

Figure 3 shows the diameters of the as-formed rPET fibers as a function of draw ratio. The average diameter

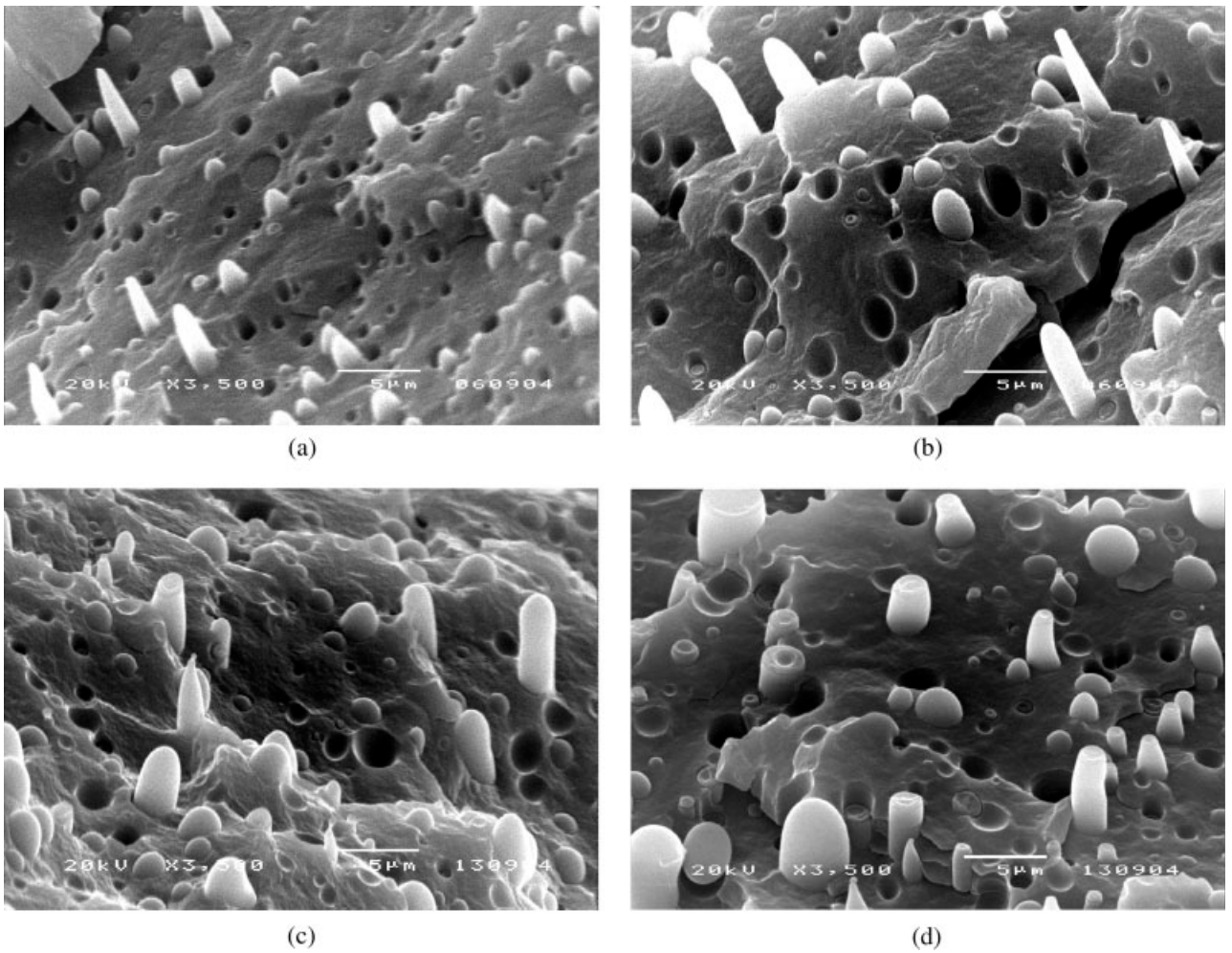

Figure 5 SEM images of cryogenic-fractured surfaces of as-extruded (a) 85/15, (b) 80/20, (c) 75/25, and (d) 70/30 w/w iPP/rPET iMFCs.

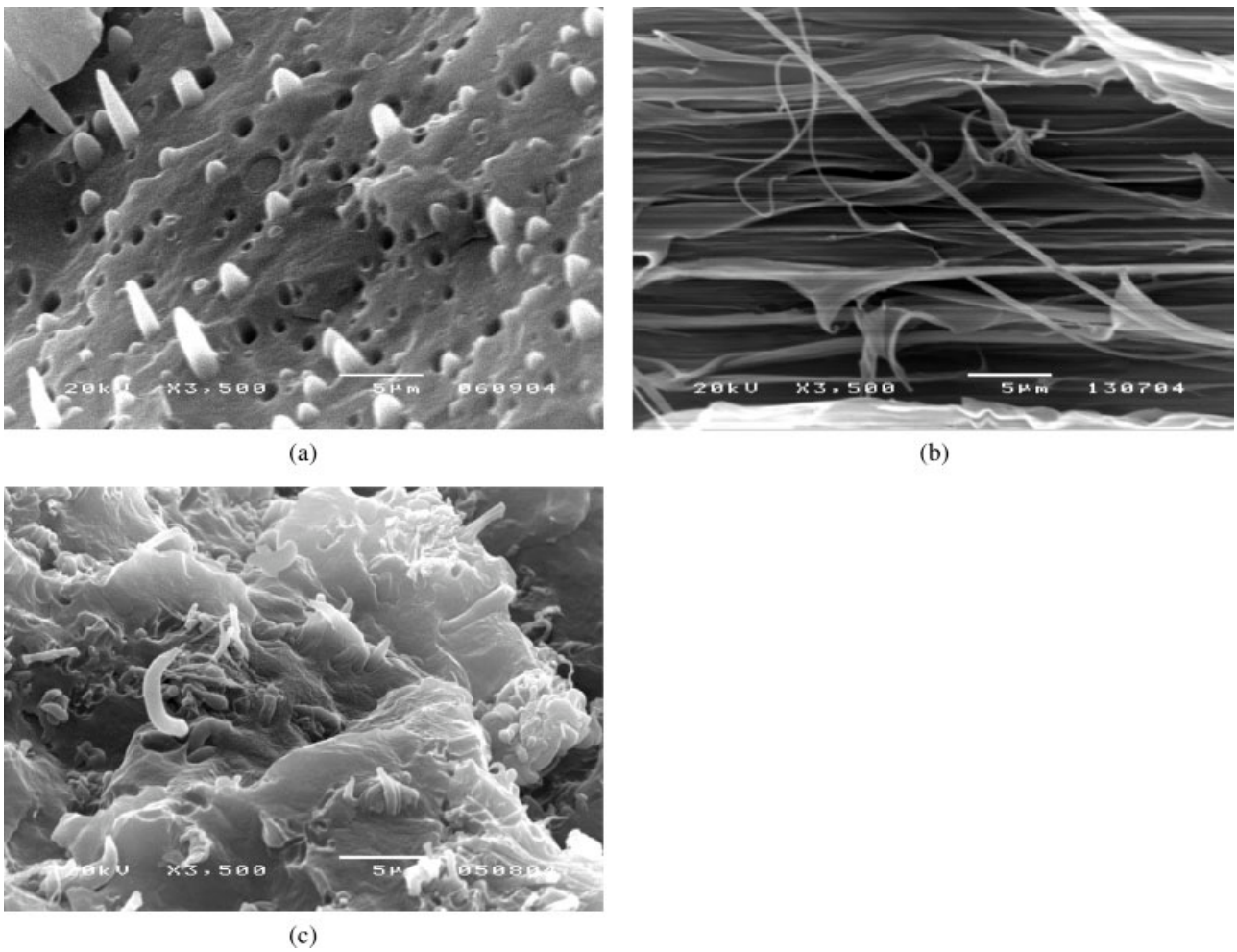

Figure 6 SEM images of fracture surfaces of (a) as-extruded (transverse), (b) as-drawn at a draw ratio of 7 (longitudinal), and (c) as-injection-molded (transverse) 85/15 w/w iPP/rPET iMFCs.

of the as-formed rPET fibers was obviously a decreasing function of the draw ratio, which is in accordance with that observed by Li et al.[10,11] Specifically, the average diameter decreased from about 1 μm for the rPET fibers formed in the neat extrudate to about 0.6 μm for the rPET fibers formed in the iPP/rPET extrudate which was drawn at the draw ratio of 2, and with further increase in the draw ratio, the average diameter decreased very gradually to reach a plateau value of about 0.4 μm at ''high'' draw ratios (5–7). The extensional stress that was applied to the extrudates caused the rPET dispersed phase to elongate to form fibers. For further investigation, the draw ratio of 7 was used. This draw ratio was chosen based mainly on the uniformity in the diameters of both the resulting iPP/rPET extrudate and the as-formed rPET fibers.

Effect of initial size of ground rPET flakes

In the grinding process, it is important to know the optimum size of ground rPET flakes that gave the best mixing efficiency with iPP in the extruder. To evaluate the effect of initial size of rPET flakes on morphological appearance of the as-formed rPET fibers and the mechanical properties of the resulting iMFCs, ground rPET flakes, sieved into 0.5–1 mm, 1–2 mm, and >2 mm size range, were investigated. For this particular investigation, the weight ratio of rPET flakes in the blends was fixed at 15 wt %. The obtained results showed that the initial size of ground rPET flakes had no effect on both the diameters of the as-formed rPET fibers and the mechanical properties of the resulting iPP/rPET iMFCs (see Table I). It can be concluded that the mixing efficiency of the extruder used in this study was good enough to achieve the same diameters of as-formed PET fibers, even when the various sizes of the ground rPET flakes were used. No difference in the mechanical properties of the resulting iPP/rPET iMFCs was observed. This is due mainly to the similar diameters of the as-formed PET fibers obtained, since it is known that the size and the shape of the dispersed phase in an incompatible polymer blend system can significantly affect the mechanical prop-

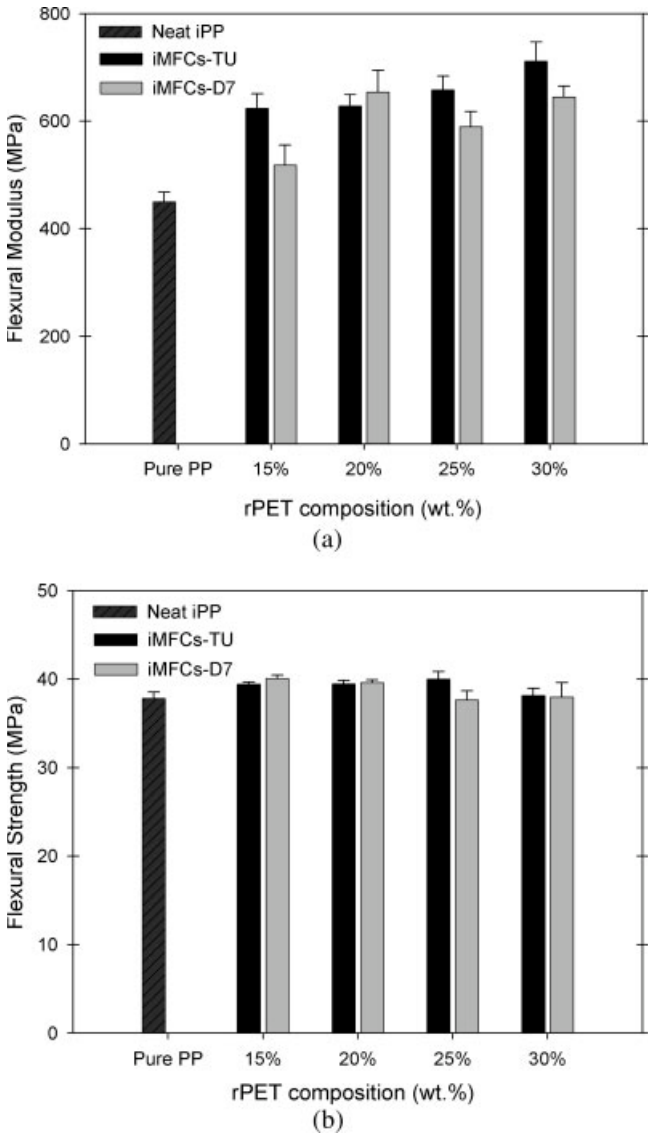

Figure 7 (a) Flexural modulus and (b) flexural strength at yield of iPP/rPET iMFCs as a function of rPET composition. Comparison was made among neat iPP, iMFCs from the as-extruded samples (iMFCs-TU), and iMFCs from the as-drawn samples (iMFCs-D7).

erties of the blends.[10,12] Based on the obtained results, rPET flakes with the initial sizes larger than 2 mm were used to prepare iMFCs for further investigation.

Effect of rPET content

Figure 4 shows diameters of the as-formed rPET fibers for three types of samples. These samples were collected at three different stages for preparing iPP/rPET iMFCs. The first type of the samples was the as-extruded samples after being passed through the home-made take-up device, the second type of the samples was the as-drawn samples (draw ratio = 7), and the last type of the samples was the as-injection-molded samples. Clearly, for each type of the samples, increasing rPET content resulted in rPET fibers of larger diameters with a wider distribution. According to Figure 5, the observed increase in the diameters of rPET fibers with increasing rPET content is evident. The most likely explanation for such an observation should be the coalescence of the rPET dispersed phase,[13] since at higher rPET contents, the possibility for adjacent rPET dispersed bodies to collide and coalesce should be increased.

More interestingly, for a given rPET content, the diameters of the rPET fibers formed in the as-extruded

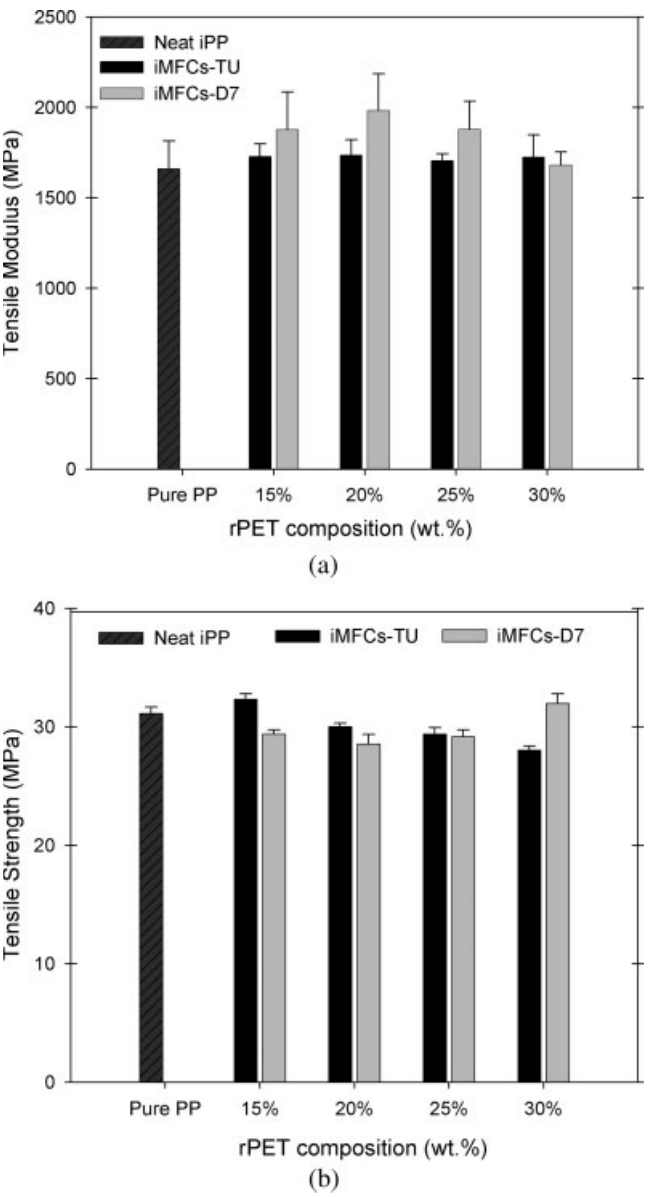

Figure 8 (a) Tensile modulus and (b) tensile strength at yield of iPP/rPET iMFCs as a function of rPET composition. Comparison was made among neat iPP, iMFCs from the as-extruded samples (iMFCs-TU), and iMFCs from the as-drawn samples (iMFCs-D7).

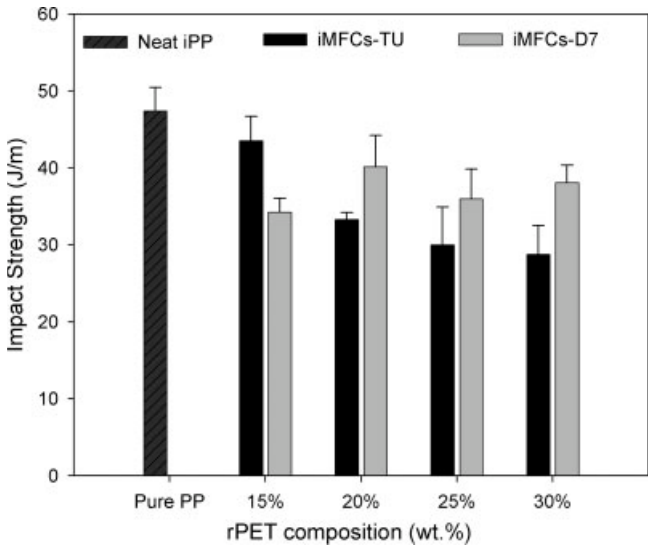

Figure 9 Impact resistance of iPP/rPET iMFCs as a function of rPET composition. Comparison was made among neat iPP, iMFCs from the as-extruded samples (iMFCs-TU), and iMFCs from the as-drawn samples (iMFCs-D7).

samples were the greatest, followed by those of the fibers formed in the as-injection-molded and the as-drawn samples (draw ratio = 7), respectively. Figure 6(a–c) show SEM images of 85/15 w/w iPP/rPET iMFCs after extrusion, drawing, and injection-molding, respectively. Clearly, rPET dispersed phase was present as fibers after extrusion [see Fig. 6(a)]. After the as-extruded samples were drawn at a draw ratio of 7, the diameters of the rPET fibers formed decreased about three times [see Fig. 6(b)], perhaps due to both the shear and extensional stresses that occurred during drawing [see Fig. 6(b)]. After the drawn samples were pelletized and later injection-molded, the rPET fibers formed after the drawing step were still perserved in the final injection-molded products [see Fig. 6(c)], with their diameters being a bit larger than those formed after the drawing step. The most likely explanation could, again, be due to the coalescence of the rPET dispersed phase.[13] Even though the nozzle temperature of 185°C was not enough to melt rPET, but it was well above the T_g of rPET of about 75°C.[10] Coupled with the fact that under the high shear and high pressure conditions during injection, the melt temperature could be even higher than the set temperature, the coalescence of the rPET dispersed phase could, therefore, occur to some extent.

Mechanical properties of iPP/rPET iMFCs were also studied. Evidently, flexural modulus of both types of iMFCs that were prepared from the as-extruded samples after being passed through the home-made take-up device (iMFCs-TU) and the as-extruded samples after being drawn at a draw ratio of 7 (iMFCs-D7) was much greater than that of neat iPP [see Fig. 7(a)]. On the other hand, the flexural strength of both types of the as-prepared iMFCs was very comparable to that of the neat iPP [see Fig. 7(b)]. For both types of the as-prepared iMFCs, the flexural modulus increased hypothetically with increasing rPET composition, with a maximum being observed for iMFCs-D7 samples at the rPET content of 20 wt %.

Tensile modulus of iMFCs-TU was slightly greater than that of neat iPP at all rPET compositions [see Fig. 8(a)]. For iMFCs-D7, only the specimens containing 15, 20, and 25 wt % rPET showed the tensile modulus greater than that of the neat iPP, with the specimens containing 20 wt % rPET exhibiting the maximum value. On the other hand, only the iMFCs-TU specimens containing 15 wt % rPET showed the tensile strength value greater than that of neat iPP, and the tensile strength of iMFCs-TU was found to decrease with increasing rPET composition [see Fig. 8(b)], most likely a result of the increase in the diameters of the as-formed rPET fibers with increasing rPET content (see Fig. 4) and the poor interfacial adhesion between the two phases as evidenced by the smooth surface of both the rPET fibers and the pull-out sites (see Figs. 5 and 6). On the other hand, only the iMFCs-D7 specimens containing 30 wt % rPET showed the tensile strength value greater than that of the neat iPP [see Fig. 8(b)].

Figure 9 shows that impact strength of all of the as-prepared iMFCs was lower than that of the neat iPP. For iMFCs-TU, the impact strength was found to monotonically decrease with increasing rPET content. On the contrary, for iMFCs-D7, the impact strength decreased appreciably from that of the neat iPP when the rPET content was 15 wt %, and, with further increase in the rPET composition, the impact strength was found to increase, with the impact strength value for the specimens having rPET content of 20 wt % being the greatest. The smaller diameters of the as-formed rPET fibers should be respon-

TABLE II
Diameters of rPET Fibers Formed in Uncompatibilized and Compatibilized iMFC Samples After Various Processing Steps

Composition of iMFCs (iPP/rPET/PP-*g*-MA)	As-extruded iMFCs (μm)	As-drawn iMFCs (μm)	As-injection-molded iMFCs (μm)
85/15/0	1.09 ± 0.23	0.38 ± 0.11	0.46 ± 0.23
85/15/2	1.02 ± 0.25	0.38 ± 0.11	0.45 ± 0.15
85/15/3	0.80 ± 0.29	0.26 ± 0.12	0.39 ± 0.11
85/15/5	0.73 ± 0.26	0.28 ± 0.11	0.40 ± 0.13
85/15/7	0.79 ± 0.28	0.29 ± 0.11	0.39 ± 0.14
70/30/0	1.52 ± 0.88	0.70 ± 0.30	0.96 ± 0.37
70/30/2	1.31 ± 0.74	0.62 ± 0.24	0.62 ± 0.21
70/30/3	1.06 ± 0.65	0.61 ± 0.27	0.62 ± 0.25
70/30/5	0.90 ± 0.41	0.64 ± 0.32	0.64 ± 0.20
70/30/7	0.83 ± 0.34	0.63 ± 0.30	0.64 ± 0.22

sible for the observed better impact resistance of iMFCs-D7 in comparison with that of iMFCs-TU. The smaller diameters of rPET fibers helped increase the impact strength by an increase in the fracture pathway, thus absorbing more energy upon failure.

Effect of PP-g-MA composition

The SEM micrographs shown in Figure 5 obviously showed the lack of interfacial adhesion between rPET fibers and iPP matrix. Li et al.[12] also reported the incompatibility of PET and iPP system. The incompatibility between rPET and iPP could be alleviated by the use of a compatibilizer.

To investigate the effect of addition and content of PP-*g*-MA which was used as the compatibilizer on the resulting iMFCs, PP-*g*-MA of varying content (i.e., 0, 2, 3, 5, or 7 wt %) was added to iPP/rPET blends to prepare compatibilized 85/15 and 70/30 w/w iPP/rPET iMFCs. For a given type of iMFC specimens, the diameters of the rPET fibers formed were found to decrease with increasing PP-*g*-MA content (see Table II). The improved interfactial adhesion between the two phases should be responsible for the observed decrease in the rPET fiber diameters. Interestingly, for iMFCs having the rPET composition of 15 wt %, the diameters of the rPET fibers formed within the as-drawn and the as-injection-molded samples did not change further when the PP-*g*-MA content was greater than or equal to 3 wt %. On the other hand, for iMFCs having the rPET composition of 30 wt %, the diameters of the rPET fibers formed within the as-drawn and the as-injection-molded samples did not change further when the PP-*g*-MA content was greater than or equal to 2 wt %.

To investigate the effect of PP-*g*-MA on the mechanical properties of the as-prepared iMFCs, injection-molded specimens for mechanical testing were obtained from the as-extruded samples after being drawn at a draw ratio of 7. The Young's modulus of the uncompatibilized 85/15 w/w iPP/rPET iMFCs was greater than that of neat iPP, while that of the compatibilized ones, regardless of the PP-*g*-MA content, was quite comparable to that of the neat iPP; and that of both the uncompatibilized and compatibilized 70/30 w/w iPP/rPET iMFCs were greater than that of the neat iPP, with the value of the compatibilized ones increasing, reaching a maximum at the PP-*g*-MA content of about 5 wt %, and decreasing with further increase in the PP-*g*-MA content (see Table III). The tensile strength of the uncompatibilized 85/15 w/w iPP/rPET iMFCs was a bit lower than that of the neat iPP. Upon addition of PP-*g*-MA, the tensile strength increased very slightly with increasing PP-*g*-MA content of up to about 3 wt %, after which it leveled off. On the other hand, the uncompatibilized 70/30 w/w iPP/rPET iMFCs showed the tensile strength slightly greater than that of the neat iPP. Upon initial addition of PP-*g*-MA, the tensile strength decreased and increased with further increase in the PP-*g*-MA content to reach a maximum value at the PP-*g*-MA content of about 5 wt % and then decreased. All of the as-prepared iMFCs exhibited the yield strain at break lower than that of the neat iPP, with the values of 70/30 w/w iPP/rPET iMFCs being lower than those of 85/15 w/w ones.

Much improvement in the mechanical properties was observed in the flexural modulus of the as-prepared iMFCs, in which both the uncompatibilized and compatibilized 85/15 and 70/30 w/w iPP/rPET iMFCs showed the property value much greater than that of the neat iPP (see Table III). All of the compatibilized 85/15 w/w iPP/rPET iMFCs had the property value much greater than that of the uncompatibilized ones, with a maximum being observed with addition of 3 wt % PP-*g*-MA, while all of the compatibilized 70/30 w/w iPP/rPET iMFCs showed the property value lower than that of the uncompatibilized ones, with the property value hypothetically decreasing with increasing PP-*g*-MA content. Furthermore, compatibilized

TABLE III
Mechanical Properties of Neat iPP and Uncompatibilized and Compatibilized 85/15 and 70/30 w/w iPP/rPET iMFCs

Composition of iMFCs (iPP/rPET/PP-*g*-MA)	Tensile properties			Flexural properties			Impact resistance (J/m)
	Modulus (MPa)	Yield strength (MPa)	Yield strain (%)	Modulus (MPa)	Yield strength (MPa)	Yield strain (%)	
100/0/0	1661 ± 153	31.1 ± 0.6	12.01 ± 0.43	450 ± 18	37.8 ± 0.7	0.31 ± 0.01	47.4 ± 3.1
85/15/0	1877 ± 96	29.4 ± 0.7	6.74 ± 2.10	518 ± 37	40.1 ± 0.4	0.33 ± 0.00	34.3 ± 1.8
85/15/2	1668 ± 43	30.7 ± 0.5	7.01 ± 0.28	579 ± 38	38.8 ± 0.8	0.29 ± 0.07	46.3 ± 3.2
85/15/3	1644 ± 56	31.0 ± 0.3	6.94 ± 0.42	624 ± 19	39.0 ± 0.7	0.27 ± 0.09	43.6 ± 2.3
85/15/5	1695 ± 39	31.2 ± 0.6	6.59 ± 0.37	592 ± 11	38.5 ± 0.8	0.27 ± 0.09	37.4 ± 2.3
85/15/7	1602 ± 23	31.1 ± 0.3	7.20 ± 0.41	595 ± 27	39.0 ± 0.7	0.32 ± 0.00	38.6 ± 2.7
70/30/0	1681 ± 74	32.0 ± 0.8	4.70 ± 0.39	645 ± 21	38.0 ± 1.6	0.13 ± 0.01	38.1 ± 2.3
70/30/2	2092 ± 104	28.4 ± 0.4	4.28 ± 0.22	623 ± 21	35.2 ± 1.0	0.13 ± 0.01	30.3 ± 1.2
70/30/3	2130 ± 92	29.6 ± 0.7	4.12 ± 0.45	632 ± 32	34.9 ± 0.4	0.13 ± 0.01	30.4 ± 1.3
70/30/5	2140 ± 81	30.1 ± 0.9	4.24 ± 0.44	622 ± 34	35.3 ± 1.3	0.13 ± 0.01	30.4 ± 2.6
70/30/7	1704 ± 114	27.9 ± 1.8	4.36 ± 0.55	613 ± 33	34.4 ± 0.8	0.13 ± 0.00	32.4 ± 2.4

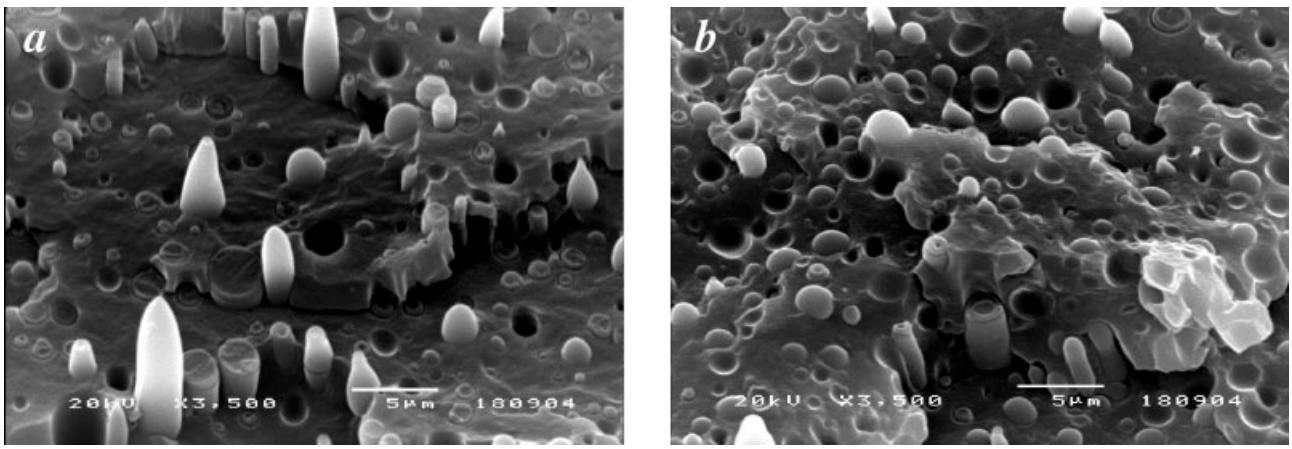

Figure 10 SEM images of cryogenic-fractured surfaces of as-extruded 70/30 iPP/rPET iMFCs compatibilized with (a) 3 and (b) 5 wt % PP-*g*-MA.

85/15 w/w iPP/rPET iMFCs showed both the flexural strength and the yield strain values comparable to or a bit greater than that of the neat iPP, while compatibilized 70/30 w/w iPP/rPET iMFCs showed the flexural strength a bit lower than that of the neat iPP, but showed the yield strain much lower than that of the neat iPP. No particular trend of these property values with PP-*g*-MA content was observed.

All of the as-prepared iMFCs showed the impact strength much lower than that of the neat iPP. For 85/15 w/w iPP/rPET iMFCs, however, initial addition of PP-*g*-MA of about 2 wt % was able to increase the property value from the uncompatibilized ones close to that of the neat iPP, but, with further addition of the compatibilizer, the property value hypothetically decreased. On the contrary, all of the compatibilized 70/30 w/w iPP/rPET iMFCs showed the property value much lower than those of the uncompatibilized ones, with the values being independent of the PP-*g*-MA content. Figure 10 shows SEM images of 70/30 w/w iPP/rPET iMFCs compatibilized by PP-*g*-MA of 3 and 5 wt %. Clearly, interfacial adhesion between the matrix and the dispersed phase did not seem to improve much, perhaps due to the low content of PP-*g*-MA in comparison with the rPET content and this could be the reason for the observed lower tensile strength, flexural strength, and impact resistance of the compatibilized 70/30 w/w iPP/rPET iMFCs in comparison with those of the uncompatibilized ones.

CONCLUSIONS

iMFCs of iPP/rPET were successfully prepared by sequential steps of melt-extrusion, drawing, and injection molding. The rPET fibers were formed by both shear and elongational stresses during extrusion through a tension provided by a home-made take-up device. The fibers were more elongated (as evidenced by the significant reduction in the fiber diameters) during hot-drawing. The average diameter of rPET fibers formed after the melt-extrusion step ranged between 1.1 and 1.6 μm, while the average diameter of rPET fibers formed after the hot-drawing step ranged between 0.4 and 1 μm, depending on the rPET composition. The initial sizes of ground rPET flakes had no particular effect on the diameters of the resulting rPET fibers and on the mechanical properties of the resulting iMFCs. An increase in the draw ratio resulted in a decrease in the diameters of rPET fibers, with a narrower distribution. Flexural modulus, tensile modulus, and tensile strength of iPP/rPET iMFCs were improved by the presence of rPET microfibers. Addition of PP-*g*-MA as the compatibilizer in the range of 2–7 wt % for this system was most suitable for the 85/15 w/w iPP/rPET iMFCs.

References

1. Evstatiev, M.; Fakirov, S.; Krasteva, B.; Friedrich, K.; Covas, J. A.; Cunha, A. M. Polym Eng Sci 2002, 42, 826.
2. Evstatiev, M.; Fakirov, S. Polymer 1992, 33, 877.
3. Cunha, A. M.; Fakirov, S. Structure Development During Polymer Processing; Kluwer: Amsterdam, 2000.
4. Evstatiev, M.; Fakirov, S.; Bechtold, G.; Friedrich, K. Adv Polym Technol 2000, 19, 249.
5. Evstatiev, M.; Fakirov, S.; Schultz, J. M.; Friedrich, K. Polym Eng Sci 2001, 41, 192.
6. Li, Z. M.; Yang, M. B.; Huang, R.; Yang, W.; Feng, J. M. Polym Plast Technol Eng 2002, 41, 19.
7. Li, Z. M.; Yang, W.; Xie, B. H.; Yang, S. Y.; Yang, M. B.; Feng, J. M.; Huang, R. Mater Res Bull 2003, 38, 1867.
8. Yoon, K. H.; Lee, H. W.; Park, O. O. J Appl Polym Sci 1998, 70, 389.
9. Tadmor, Z.; Gogos, G. Principles of Polymer Processing; Wiley: New York, 1979.
10. Li, Z. M.; Yang, M. B.; Xie, B. H.; Feng, J. M.; Huang, R. Polym Eng Sci 2003, 43, 615.
11. Li, Z. M.; Xie, B. H.; Huang, R.; Fang, X. P.; Yang, M. B. Polym Eng Sci 2004, 44, 2165.
12. Li, Z. M.; Li, L. B.; Shen, K. Z.; Yang, M. B.; Huang, R. J Polym Sci Part B: Polym Phys 2004, 42, 4095.
13. Li, Z. M.; Yang, W.; Huang, R.; Fang, X. P.; Yang, M. B. Macromol Mater Eng 2004, 289, 426.